

left to right along the helical groove. In the  $\lambda$  isomer this same vector is directed from right to left opposing the right-handed groove. This structural difference between the enantiomers leads to unfavorable contacts between the nonintercalating ligands on the  $\lambda$  isomer and the sugar phosphate backbone of the DNA double helix. Because the presence of the phenyl groups increases the number of these potential contacts, this model would account for the increase in chiral discrimination observed for  $\text{Ru}(\text{DIP})_3^{2+}$  in comparison to that for  $\text{Ru}(\text{phen})_3^{2+}$ . Thus, this model may be useful both for designing new experiments and for developing new DNA binding agents of high site and conformation specificity.

**Acknowledgment.** This research was supported by the National Institutes of Health through Grants GM21589 (H.M.B.), CA06927 (H.M.B.), CA09035 (B.M.G.), RR05539 (H.M.B.), and GM33309 (J.K.B.) and through an appropriation from the Commonwealth of Pennsylvania. We thank Avis Danishefsky for preparation of the complex.

**Registry No.**  $[\text{Ru}(\text{DIP})_3]\text{Cl}_2$ , 36309-88-3.

**Supplementary Material Available:** Listings of observed and calculated structure factors and thermal parameters for  $\text{Ru}(\text{DIP})_3^{2+}$  (18 pages). Ordering information is given on any current masthead page.

Contribution from the Department of Chemistry, Rutgers,  
The State University of New Jersey, New Brunswick, New Jersey 08903

## Light-Induced Excited-Spin-State Trapping: Evidence from VTFTIR Measurements

R. Herber\* and L. M. Casson

Received July 23, 1985

Samples of *cis*- $\text{Fe}(\text{phen})_2(\text{SCN})_2$  (phen = 1,10-phenanthroline) were examined by variable-temperature Fourier transform infrared spectroscopy over the range  $8 \leq T \leq 310$  K. The room-temperature high-spin form and the low-spin form stable at liquid-nitrogen temperature can be readily distinguished by their characteristic infrared signatures, both in the  $\nu_{\text{CN}}$  region ( $\sim 2100$   $\text{cm}^{-1}$ ) and in the spectral range 900–600  $\text{cm}^{-1}$ . The high-spin–low-spin conversion in KBr as estimated from infrared intensities is approximately half-complete at  $159 \pm 5$  K, a temperature  $\sim 20$  K lower than that extracted from heat capacity, susceptibility, and  $^{57}\text{Fe}$  Mössbauer data. When the sample is cooled to  $\sim 8$  K, the low-spin form of the complex is converted to a high-spin form by optical pumping due to the 632.8-nm radiation of the He/Ne laser of the spectrometer. The high-spin form so produced by the LIESST process is stable in KBr, CsI, and TlBr matrices at low temperatures but is gradually transformed into a low-spin form on warming the samples above  $\sim 32$  K. Both the thermodynamics and kinetics of the conversion processes between the several spin states of the ferrous complex can be conveniently followed by infrared spectroscopic techniques.

### Introduction

The phenomenon of thermally driven spin crossover in first-row transition-metal complexes, with electron configurations  $d^4$  to  $d^7$ , which was first demonstrated in tris(dithiocarbamate) complexes of  $\text{Fe}^{3+}$  by Cambi et al.,<sup>1</sup> has been extensively reviewed in the literature. In particular, the  $^5\text{T}_2$  (high-spin, HS)<sup>–1</sup>A (low-spin, LS) transition in *cis*- $\text{Fe}^{\text{II}}(\text{phen})_2(\text{SCN})_2$  has been studied in considerable detail by Gutlich et al.,<sup>2–5</sup> who have made use of  $^{57}\text{Fe}$  Mössbauer spectroscopy and susceptibility measurements to characterize the temperature dependence of the transition from the  $S = 2$  to the  $S = 0$  configuration of the complex. The magnetic behavior of  $\text{Fe}(\text{phen})_2(\text{SCN})_2$  had been originally observed by Baker and Bobonich,<sup>6</sup> who noted that the spin transition is very sharp and occurs at  $\sim 175$  K in the solid, with little or no hysteresis during warming and cooling cycles. In particular it is interesting to note that not only is there the expected characteristic susceptibility difference between the HS and LS form of this compound but in addition both the Mössbauer and infrared signatures of the two spin states are significantly different and permit a detailed study of the thermodynamics of the crossover phenomenon. The

relevant temperature-dependent data, especially as they pertain to the Mössbauer studies, have recently been reviewed by Gutlich.<sup>5,7</sup>

From such studies, it has become clear that if the subject samples are carefully prepared and treated prior to spectroscopic or susceptometric examination, complete conversion of the room-temperature HS form of  $\text{Fe}(\text{phen})_2(\text{SCN})_2$  to the LS form can be achieved on cooling to liquid-nitrogen temperature. Of particular interest is the observation by Mössbauer techniques<sup>8–10</sup> that when the LS form is irradiated with white light at temperatures below  $\sim 50$  K, a conversion to a form that has the Mössbauer spectral characteristics of the HS form can be achieved. This HS form, in turn, can be reconverted to the LS form by annealing the samples at temperatures of 30–32 K for short time periods. On recooling such annealed samples to liquid-helium temperatures in the dark, only the LS form spectroscopic parameters are observed. These transitions are schematically summarized in Figure 1, in which it is seen that the room-temperature form (HS-1) converts to the low-spin form (LS-1) on cooling to  $\sim 100$  K. Further cooling, in the absence of optical excitations, to liquid-helium temperature, preserves the LS-1 form, which can then be converted to a high-spin form (HS-2) by optical pumping. When this metastable system is warmed above  $\sim 30$  K, a reversion to a low-spin form (LS-2), which is stable at  $\sim 100$  K, is observed.

- (1) Cambi, L.; Cagnasso, A. *Atti. Accad. Naz. Lincei, Cl. Sci. Fis., Mat. Nat., Rend.* **1931**, *13*, 809. Cambi, L.; Szego, L. *Ber. Dtsch. Chem. Ges. B* **1931**, *64*, 259.
- (2) Gutlich, P. *Struct. Bonding (Berlin)* **1981**, *44*, 83. See also the review by: König, E.; Ritter, G.; Kulshretha, S. K. *Chem. Rev.* **1985**, *85*, 219 and references therein.
- (3) Müller, E. W.; Spiering, H.; Gutlich, P. *Chem. Phys. Lett.* **1982**, *93*, 567.
- (4) Ganguli, P.; Gutlich, P.; Müller, E. W.; Irlner, W. *J. Chem. Soc. Dalton* **1981**, 441.
- (5) Gutlich, P. In "Mössbauer Spectroscopy Applied to Inorganic Chemistry", Vol. 1, Long, G. J., Ed.; Plenum Press: New York, 1984; Vol. 1, Chapter XI, and references therein.
- (6) Baker, W. A.; Bobonich, H. M. *Inorg. Chem.* **1964**, *3*, 1184.

- (7) Gutlich, P. In "Chemical Mössbauer Spectroscopy"; Herber, R. H., Ed.; Plenum Press: New York, 1984; Chapter II.
- (8) Decurtins, S.; Gutlich, P.; Kohler, C. P.; Spiering, H. *Chem. Phys. Lett.* **1984**, *105*, 1; *J. Chem. Soc. Chem. Commun.* **1985**, 430.
- (9) Decurtins, S.; Gutlich, P.; Hauser, A.; Hasselbach, K. M.; Spiering, H. *Inorg. Chem.* **1985**, *24*, 2174.
- (10) Decurtins, S.; Gutlich, P.; Kohler, C. P.; Spiering, H. *J. Chem. Soc., Chem. Commun.* **1985**, 430.

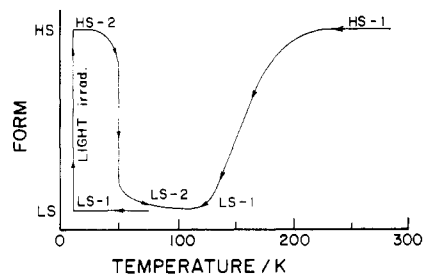


**Figure 1.** Schematic diagram for the successive conversion of  $\text{Fe}(\text{phen})_2(\text{SCN})_2$  from the high-spin (HS) to the low-spin (LS) forms discussed in the text.

As has been noted by Baker and Long,<sup>11</sup> Teodorescu,<sup>12</sup> and Maddock et al.,<sup>13</sup> inter alia, the infrared signatures of the HS and LS forms are sufficiently different to permit a ready identification of the form of  $\text{Fe}(\text{phen})_2(\text{SCN})_2$  that is present under a given set of conditions by the use of infrared spectroscopic techniques. The recent development of variable-temperature Fourier transform infrared spectroscopy (VTFTIR) as a sensitive tool for the study of the thermal behavior of covalent solids has made it possible to study in detail the vibrational properties of spin-transition compounds as a function of temperature. In particular, it is possible to address the question of whether the two high-spin forms, HS-1 and HS-2 (Figure 1), and the two low-spin forms, LS-1 and LS-2, are in fact identical, and to follow both the thermodynamics and kinetics of the conversion processes among the several spin states, in detail. The results of such a study, which has also served to demonstrate unambiguously the LIESST phenomenon<sup>8,14,15</sup> in  $\text{Fe}(\text{phen})_2(\text{SCN})_2$  at 8 K as a result of He/Ne laser pumping, are discussed in the present communication.

### Experimental Section

**(a)  $\text{Fe}(\text{phen})_2(\text{SCN})_2$ .** A number of synthetic procedures for preparing this compound have been reported in the literature,<sup>16,13</sup> and as pointed out by Gutlich et al.,<sup>7</sup> the completeness and details of the temperature dependency of the spin-crossover phenomenon appear to depend not only on the quality of the solid obtained by the synthetic route used but also on the subsequent treatment of the samples in question. In the present study, use has been made of the aqueous procedure of Schilt and Fritsch,<sup>17</sup> in which solutions of ferrous ammonium sulfate and 1,10-phenanthroline are acidified with  $\text{H}_2\text{SO}_4$ , followed by the addition of KSCN. This procedure immediately produces a reddish precipitate, which according to Maddock et al.<sup>13</sup> is best formulated as  $[\text{Fe}(\text{phen})_3]_2[\text{Fe}(\text{NCS})_4][\text{NCS}]_2 \cdot 3\text{H}_2\text{O}$  and which shows a susceptibility of  $2.68 \mu_B$  at room temperature. This precipitate rapidly changes color on standing in contact with the supernate to a deep red-violet and settles out from the solution after occasional shaking, when allowed to "age" for 24 h. The "aged" precipitate was filtered, washed with a small quantity of deionized water, and then air-dried. As noted by Maddock et al.,<sup>13</sup> conversion of this product to the desired anhydrous cis compound can be effected by treatment with appropriate organic solvents. Complete conversion to the anhydrous cis form was effected in the present investigation by a 60-h reflux in acetonitrile (bp  $81.6^\circ\text{C}$ ), or pyridine (bp  $115.5^\circ\text{C}$ ) and drying in vacuo over  $\text{P}_2\text{O}_5$  at  $90^\circ\text{C}$ . These products are identified as FeAC and FePY, respectively, in the subsequent discussion. Anal. Calcd for  $\text{Fe}(\text{C}_{26}\text{H}_{16}\text{N}_6\text{S}_2)_2$ : C, 58.65; H, 3.03; N, 15.79. Found for FeAC: C, 57.37; H, 2.82; N, 15.36. Found for FePY: C, 57.43; H, 3.09; N, 15.41. Both of these samples were found to be identical with a sample of *cis*- $\text{Fe}(\text{phen})_2(\text{SCN})_2$  that had been used in previous Mossbauer effect studies.<sup>18</sup> The approximately  $34^\circ\text{C}$  difference in the reflux

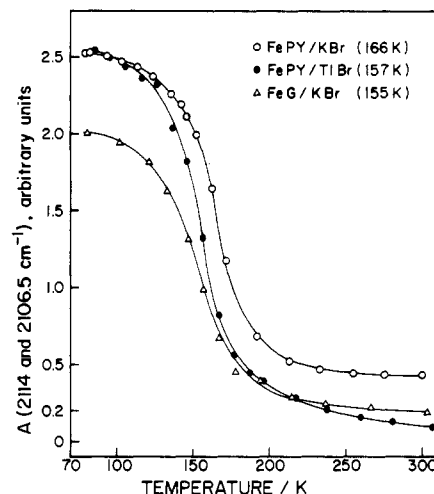


**Figure 2.** Temperature dependence of the infrared absorbance at 2114 and  $2106.5 \text{ cm}^{-1}$  associated with the LS form of  $\text{Fe}(\text{phen})_2(\text{SCN})_2$ . The temperatures at which the intensity sum reaches its mean value between 80 and 300 K are shown in parentheses and have an estimated uncertainty of  $\pm 5^\circ$ .

temperatures of the two solvents used does not produce any detectable differences in the properties of the resultant products. The  $^{57}\text{Fe}$  Mössbauer parameters of FePY and FeAC are identical, within experimental error, with the values reported by Gutlich et al. at 300 and 77 K.

Pellets for spectroscopic study were prepared by variations on the following theme: KBr, CsI, or TlBr were thoroughly dried under vacuum and then pulverized by using a 2-mL plastic capsule-and-ball shaking arrangement for 50 s. The sample compound was added to this powder to give  $\sim 0.2$ –1% solute by weight. This mixture was shaken for 5 s, transferred to an evacuable pellet die, pumped out to a pressure of  $\sim 10 \mu\text{m}$ , and then pressed at  $10000 \text{ lb in}^{-2}$  to give a clear pellet. Longer or shorter mixing times or pressing at lower pressures gave less satisfactory results.

**(b) Spectrometer.** The midrange IR data herein reported were acquired on an IBM/32 FTIR nitrogen-purged instrument, provided with a DTGS detector. Typically, 30–100 interferometer scans were coadded and ratioed to a background acquired with the sample cell (vide infra) containing a pellet of the appropriate matrix (KBr, CsI, or TlBr) as a blank. Absorption maxima were located by using the PEAKPICK software or by manual cursor movement, as appropriate. The nominal spectrometer resolution is  $2 \text{ cm}^{-1}$ . The precision in determining band positions is  $\pm 0.5 \text{ cm}^{-1}$ .

**(c) Sample Cell and Temperature Control.** The Invar low-temperature cell used in the present study has been described previously.<sup>19</sup> Two minor modifications used were the addition of a small amount of CRYOCON grease in seating the sample pellet into the sample cell to insure good thermal contact and the addition of an  $\sim 500\text{-}\Omega$  Allen Bradley  $1/4\text{-W}$  carbon resistor to monitor the sample temperature below  $\sim 30 \text{ K}$ . To effect the latter, use was made of the Lindenfeld universal calibration curve<sup>20</sup> for such resistors used as low-temperature thermometers.

### Results and Discussion

**(a) The  $\sim 2100$ – $2000\text{-cm}^{-1}$  Region.** The infrared spectra of ferrous phenanthroline complexes have been reported by numerous investigators.<sup>11</sup> The most complete assignments are those of König and Madeja<sup>21</sup> who report band positions at both 298 and 105 K. Two regions accessible with a midrange spectrometer are especially useful for examining the spin-crossover phenomena in such solids. As already noted in the early communications by Baker and Long,<sup>11</sup> the  $\nu_{\text{CN}}$  region from 2200 to  $2000 \text{ cm}^{-1}$  permits a clear distinction between the HS form (strong bands at 2057 and  $2070 \text{ cm}^{-1}$ ) and the LS form (absorptions at 2110 and  $2103 \text{ cm}^{-1}$ ) to be made. These spectral characteristics have also been discussed

- (11) Baker, W. A., Jr.; Long, G. J. *Chem. Commun.* **1965**, 15, 368.
- (12) Teodorescu, M. *Rev. Roum. Chim.* **1976**, 21, 7; Spacu, P., Teodorescu, M.; Ciomartan, D. *Ibid.*, **1967**, 12, 145.
- (13) Savage, S.; Jia-Long, Z.; Maddock, A. G. *J. Chem. Soc., Dalton Trans.* **1985**, 991.
- (14) McGarvey, J. J.; Lawthers, I. J. *J. Chem. Soc., Chem. Commun.* **1982**, 906.
- (15) The term "light-induced excited-spin-state trapping" (LIESST) in connection with studies of a number of Fe(II) complexes was first introduced by Gutlich et al.; see ref 7 and citations therein.
- (16) Madeja, K.; König, E. *J. Inorg. Nucl. Chem.* **1963**, 25, 377. Madeja, K.; Wilke, W.; Schmidt, S. *Z. Anorg. Allg. Chem.* **1966**, 346, 306.
- (17) Schilt, A. A.; Fritsch, K. *J. Inorg. Nucl. Chem.* **1966**, 28, 2677.
- (18) The authors are indebted to Prof. P. Gutlich for generously making this sample available for the purposes of the comparisons cited herein.

- (19) Casson, L. M.; Herber, R. H. *Rev. Sci. Instrum.* **1985**, 56, 1593. Casson, L. M.; Herber, R. H. "Proceedings, 1985 International Conference on Fourier and Computerized Infrared Spectroscopy, Ottawa, June 1985". *Proc. SPIE—Int. Soc. Opt. Eng.* **1985**, 553, 478.
- (20) Lindenfeld, P. *Temp. Its Meas. Control Sci. Ind.* **1962**, 3, 399.
- (21) König, E.; Madeja, K. *Spectrochim. Acta, Part A* **1967**, 23A, 45. See also: König, E. *Coord. Chem. Rev.* **1968**, 3, 471.

by Sorai and Seki,<sup>22</sup> who were able to demonstrate the progressive disappearance of the absorptions due to the HS form as the temperature is reduced to 88 K. At the lowest temperature reported by them, the HS fraction, as judged from the IR band peak areas, is  $\sim 1.5\%$ . These results have been amply confirmed in the present study, in which it was observed that the HS infrared doublet absorption (at 2072 and 2063  $\text{cm}^{-1}$ ) decreases in intensity, with the concomitant growth of the LS absorptions (at 2114 and 2106.5  $\text{cm}^{-1}$ ), as the temperature is lowered to that of liquid nitrogen, without any significant temperature-dependent shift of the band positions over the whole temperature range.

The temperature dependence of the total intensity of the LS absorptions at 2114 and 2106.5  $\text{cm}^{-1}$  is summarized graphically in Figure 2. These results are in good agreement with those reported by Baker and Long,<sup>11</sup> who presumably employed a dispersive infrared spectrometer in their studies (no information on the physical form of their samples is given). In all three cases, the midpoint of the apparent  $\text{HS} \rightleftharpoons \text{LS}$  crossover, as judged by the IR data, is observed at  $159 \pm 5$  K, a temperature which is significantly lower than the transition temperature of 176.29 K extracted from the specific heat data of Sorai and Seki,<sup>22,23</sup> the value of 174 K reported by König and Madeja<sup>24</sup> and by Baker and Bobonich<sup>25</sup> on the basis of susceptibility studies, and the values reported by Gutlich and his co-workers based on  $^{57}\text{Fe}$  Mössbauer quadrupole splitting and line width data.<sup>3,7</sup> The latter authors have also noted the dependence of the  $\text{HS} \rightleftharpoons \text{LS}$  conversion temperature dependence on crystal quality and sample treatment. Since infrared bands show considerable sharpening at low temperature, and thus there is no direct correlation between the concentrations of absorber moieties and absorption intensity, it is not clear what particular significance can be attached to the differences noted in the intensity of the  $\sim 2100\text{-cm}^{-1}$  absorption and  $T_c$  as determined by other physicochemical techniques. What is significant in the context of the present discussion is the fact that the inflection point of the LS infrared band temperature-dependent intensity curve is significantly lower than that corresponding to the heat capacity, susceptibility, and Mössbauer data. In connection with the latter, it is interesting to note that the sample of  $\text{Fe}(\text{phen})_2(\text{SCN})_2$  (FeG) provided by Prof. Gutlich,<sup>18</sup> which had been used in the earlier  $^{57}\text{Fe}$  Mössbauer studies, gave results essentially identical with those observed with the samples synthesized in the source of this study. Finally, from the data summarized in Figure 2, it is noted that the temperature dependence of the IR intensity is matrix independent to a reasonably good approximation, as expected.

The data summarized in Figure 2 further show that it is possible to use the  $\text{HS} \rightleftharpoons \text{LS}$  conversion as a sensitive "thermometer" to estimate sample heating in the infrared beam of the spectrometer. As the nominal sample temperature was held constant at  $155.5 \pm 0.1$  K (near the point of maximum change in the absorption intensity due to the LS-1 form), two filters were inserted successively in the sample compartment, "upstream" from the sample position. The first of these was an absolute filter (A1), which blocked both the infrared and laser radiation incident on the sample. This filter was in situ 90% of the time, being removed only for 1-min intervals every 10 min to permit accumulation of a sample spectrum. The second filter was a "blue" filter prepared from 6 layers of 1.18  $\text{mg}/\text{cm}^2$  Saran wrap, coated on both sides with a blue dye having an absorption maximum at  $\sim 635$  nm (vide infra, Figure 4). This blue filter blocked the He/Ne laser radiation, but permitted transmission of the infrared beam to effect data collection. Interposition of either of these filters left the ratio of the absorption intensity of the HS-1 form (2074 and 2062  $\text{cm}^{-1}$ ) invariant within  $\pm 1\%$  or better compared to the "no filter" data showing that sample heating from either radiation source is negligible in terms of the  $\text{HS} \rightleftharpoons \text{LS}$  equilibrium under the experimental conditions employed.

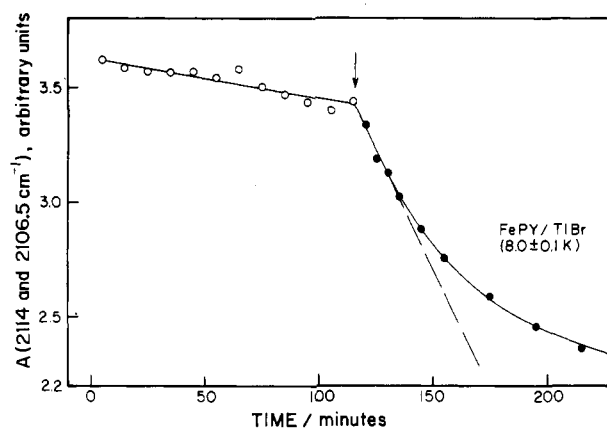


**Figure 3.** Conversion of the LS-1 form of  $\text{Fe}(\text{phen})_2(\text{SCN})_2$  to the HS-2 form (see text) at  $8.0 \pm 0.1$  K under the influence of the 632.8-nm He/Ne laser irradiation. In the interval  $5 \leq t \leq 115$  min, the absolute shutter was removed 10% of the time for data accumulation. At  $t = 120$  min this shutter was completely removed. The dashed line indicates the initial (linear) slope of the rate of the intensity sum change. The ratio of the two slopes is  $\sim 10:1$ .

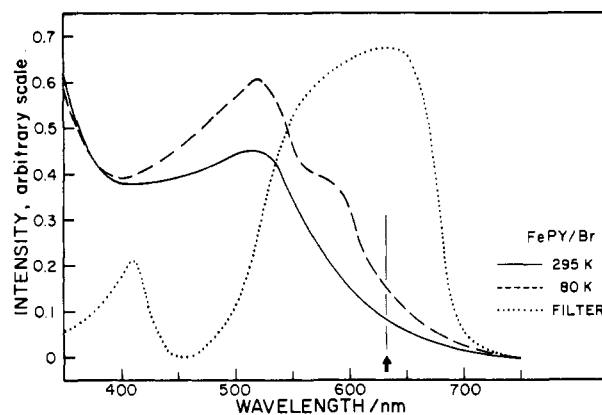


**Figure 4.** Absorption spectrum of  $\text{Fe}(\text{phen})_2(\text{SCN})_2$  at 295 K (solid line) and at  $\sim 80$  K (dashed line). The absorption of the blue filter discussed in the text is indicated (dotted line), as is the position of the emission line of the He/Ne laser used in the spectrometer (arrow).

Thus, the difference between the inflection point of the infrared absorptions ( $\sim 159 \pm 5$  K) and the transition temperature ( $175 \pm 1$  K) reported earlier<sup>7,22-25</sup> cannot be ascribed to sample heating effects and remains incompletely understood on the basis of the present data.<sup>28</sup>

In consonance with the observations of Gutlich et al.<sup>11</sup> related to crystal quality/sample treatment effects, it should be noted that in all three matrices used in the present study, some absorption intensity in the 2080–2060- $\text{cm}^{-1}$  region, ascribed to the HS form, coexists even at 80 K. In an effort to determine whether this observation arises from inadequate temperature lowering of the complex, the samples were cooled further to  $\sim 8\text{--}10$  K. Surprisingly, it was noted that the absorption assigned to the HS form not only did not decrease further beyond its value at 80 K but in fact showed a time-dependent increase, accompanied by a parallel decrease of the intensity of the absorptions at  $\sim 2100\text{-cm}^{-1}$  associated with the LS form of the complex. This initially unexpected result can be readily understood on the basis of the

(26) Melick, D.; Herber, R. H. "Proceedings, 1985 International Conference on Fourier and Computerized Infrared Spectroscopy, Ottawa, June 1985". *Proc. SPIE—Int. Soc. Opt. Eng.* **1985**, 553, 400. Melick, D. Senior Honors Research, Rutgers University, May 1985.

(27) Herber, R. H. *Polyhedron* **1985**, 4, 1969.

(28) One of the reviewers has suggested two possible explanations for these observations relating (a) to the pelletizing process in which a pressure of 20000 lb  $\text{in}^{-2}$  is exerted on the KBr matrix and (b) to the dilution of the sample compound in KBr. The implications of both of these suggestions are being investigated in this laboratory at the present time.

(22) Sorai, M.; Seki, S. *J. Phys. Chem. Solids* **1974**, 35, 555.

(23) Sorai, M.; Seki, S. *J. Phys. Soc. Jpn.* **1972**, 33, 575.

(24) König, E.; Madeja, K. *Inorg. Chem.* **1967**, 6, 48.

(25) Baker, W. A., Jr.; Bobonich, H. M. *Inorg. Chem.* **1964**, 3, 1184.

light-induced excited-spin-state trapping (LIESST) phenomenon, first suggested by McGarvey<sup>14</sup> and developed in persuasive detail by Gutlich et al. In this process, optical pumping at the LS form of the complex ( $^1A_1$ ) populates a number of excited-state levels that can decay by intersystem crossing to a low-lying level of the  $^5T$  manifold, which is then energetically trapped at low temperatures. The stability of this trapped HS form of  $\text{Fe}(\text{phen})_2(\text{SCN})_2$  at temperatures near that of liquid helium, and the subsequent reconversion to an LS form on warming above  $\sim 30$  K, has been clearly demonstrated in the  $^{57}\text{Fe}$  Mössbauer experiments that have been reported. An obvious question that arises in this connection is as follows: In the absence of the intense white light sources used in the low-temperature LIESST  $^{57}\text{Fe}$  Mössbauer experiments,<sup>8</sup> what causes the optical pumping at  $\sim 10$  K in the infrared spectrometer used in the present studies? There are, in fact, two radiation sources in this spectrometer that result in a photon flux at the sample position. One of these is the infrared beam emitted by the ceramic element source, operated at a temperature of  $\sim 1315$  °C; the other is a very low-power ( $\sim 0.5$  mW) He/Ne laser used to generate the calibration for the interferometer pattern on which the Fourier transform mode of operation is predicated. These two beams are colinear at the convergence point of the IR beam in the sample compartment. The IR beam diameter is  $\sim 35$  mm; the sample pellet diameter is  $\sim 13$  mm. The laser beam is concentrated primarily at the center of the pellet. A simple experiment can distinguish between these two possible sources of optical-pumping radiation in the present experiment. When the absolute shutter is interposed in the sample beam (being removed only to effect data acquisition) a very slow rate of LS  $\rightarrow$  HS conversion is observed when the residual blue filter is retained in the optical path. When the blue filter is removed, the LS  $\rightarrow$  HS conversion (as judged by the diminution in the absorption intensity of the 2114- and 2107- $\text{cm}^{-1}$  bands) is significantly increased. These observations are summarized graphically in Figure 3, from which it is seen that when the sample is exposed to the laser frequency radiation for 10% of the time, the conversion rate is slow, whereas when the sample is continuously exposed to the 632.8-nm He/Ne line, the LS  $\rightarrow$  HS conversion is much more rapid. The ratio of the two slopes (using the initial slope after removal of the shutter) is  $0.10 \pm 0.05$ , in good agreement with the ratio of "exposure" times, which is  $0.11 \pm 0.01$ .

The rate of the LS  $\rightarrow$  HS conversion at  $8 \pm 1$  K after removal of the shutter does not follow exactly the first-order kinetics that might have been expected from first principles, as is evidence from the fact that a plot of  $\log(\text{absorbance})$  vs. time does not yield a linear function. This observation is presumably due to the fact that the sample does not consist of a homogeneously dispersed absorber, but rather of aggregates of varying size (and thickness) in the dispersant matrix. These results do, however, provide an additional clue not readily extractable from the white light irradiation procedures reported by Gutlich et al.; namely that the LS  $\rightarrow$  HS conversion at low temperature is not due to local heating effects, but rather arises from the optical-pumping mechanism postulated earlier. The temperature of the Invar sample cell, which intercepts both the IR and He/Ne laser irradiation, is readily monitored at low temperatures from the data on the Allen Bradley resistor described above. The temperature so monitored was the same within  $\pm 0.1^\circ$  with and without interposition of the shutter, pointing to an optical rather than a thermal mechanism for the LS  $\rightarrow$  HS conversion at low temperatures.

From these results the obvious question arises: Is the absorption spectrum of *cis*- $\text{Fe}(\text{phen})_2(\text{SCN})_2$  such that the He/Ne laser radiation can indeed excite the metal-to-ligand charge-transfer band? The visible absorption spectrum of the sample compound, dispersed in a KBr matrix, is shown graphically in Figure 4, which includes data at 295 and  $\sim 80$  K as well as the absorption spectrum of the blue filter used in the experiments described above. The room-temperature spectrum shows a broad maximum at  $\sim 520$  nm ( $19\,230\text{ cm}^{-1}$ ) while the 80 K spectrum shows an additional shoulder at  $\sim 585$  nm ( $17\,090\text{ cm}^{-1}$ ). The absorptions at the He/Ne laser line ( $15\,800\text{ cm}^{-1}$ ) while weak, are sufficiently large to permit optical pumping to the metal-to-ligand charge-transfer

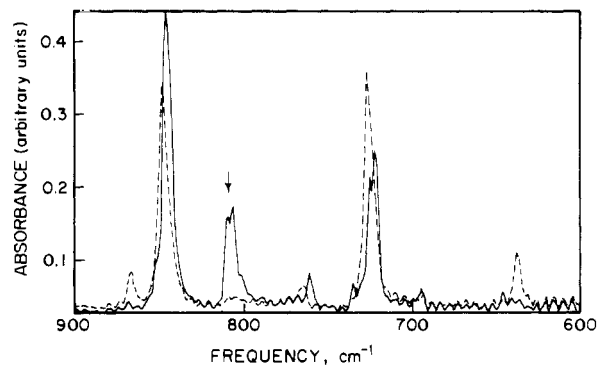


**Figure 5.** Infrared absorption spectrum of  $\text{Fe}(\text{phen})_2(\text{SCN})_2$  in the 900–600- $\text{cm}^{-1}$  region. The dashed line refers to a sample temperature of  $300 \pm 1$  K and the solid line to a sample temperature of  $80 \pm 1$  K. The absorbances at 803  $\text{cm}^{-1}$  ( $\nu_{\text{CS}}$  of the SCN ligand) and that at 637  $\text{cm}^{-1}$  ( $\gamma_{\text{CCC}}$ , in plane ring deformation) were used in the temperature-dependence data summarized in Figure 6.

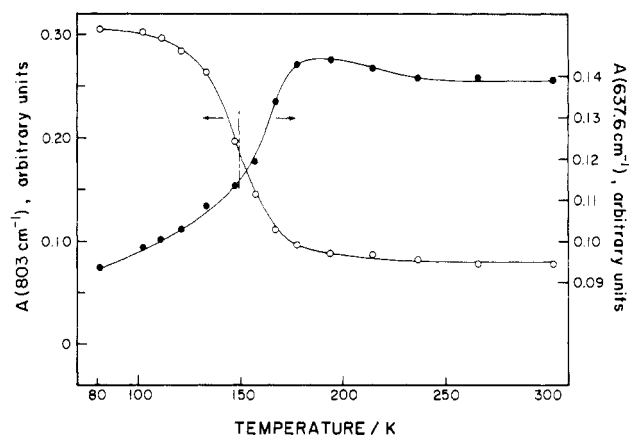


**Figure 6.** Temperature dependence of the infrared absorbances at 803 and 637  $\text{cm}^{-1}$  associated with the conversion between the HS-1 and LS-1 forms (see text and Figure 1) of  $\text{Fe}(\text{phen})_2(\text{SCN})_2$ . The vertical dashed line shows the temperature at which the mean absorbance value in the range 80–300 K is reached.

band in the  $^1A_1$  manifold, as suggested by Gutlich,<sup>10</sup> especially at the lower temperature. Moreover, the data summarized in Figure 4 clearly show the efficacy of the blue filter, used to reduce the rate of the LS  $\rightarrow$  HS conversion, as discussed above. These results confirm directly the assumption that the optical pumping in the  $^1A_1$  manifold can be ascribed to the He/Ne laser of the infrared spectrometer.

**(b) The 900–600- $\text{cm}^{-1}$  Region.** In addition to the  $\nu_{\text{CN}}$  region of the midrange infrared spectrum, the 900–600- $\text{cm}^{-1}$  region can be used to identify and characterize the ferrous phenanthroline complexes under discussion. In their recent communication, Maddock et al.<sup>13</sup> have pointed out that a major difference between the IR spectra of *cis*- $\text{Fe}(\text{phen})_2(\text{SCN})_2$  and the "red compound" discussed by them is the presence of medium-intensity bands at 866 and 637  $\text{cm}^{-1}$  in the former, and two weak features at 643 and 610  $\text{cm}^{-1}$  in the latter. In addition, the "red compound" exhibits a moderately strong, broad absorption at  $\sim 770\text{ cm}^{-1}$ , while in the subject compound this band is split into two weak features at  $\sim 806$  and  $764\text{ cm}^{-1}$ . Representative spectra of  $\text{FePY}$  in KBr in this region at  $300 \pm 1$  and  $80 \pm 1$  K are shown in Figure 5. From the assignments of König and Madeja,<sup>21</sup> the strong absorptions at 847 and 725  $\text{cm}^{-1}$  are due to  $\gamma(\text{CH})$  out-of-plane motions while the band at 638  $\text{cm}^{-1}$  is due to an in-plane ring deformation and might not be expected to be sensitive to the spin state of the metal atom. On the other hand, the weak absorption at  $\sim 806\text{ cm}^{-1}$  is assigned to  $\gamma_3$ , the C–S stretch of the thiocyanate group. The 865- $\text{cm}^{-1}$  feature is unassigned. Both of these latter two absorptions, as well as the 638- $\text{cm}^{-1}$  feature, undergo significant changes, as shown in Figure 6, with the  $\sim 806\text{-cm}^{-1}$  band becoming more intense, while the absorptions at 865 and 637  $\text{cm}^{-1}$

**Table I.** Infrared Bands of  $\text{Fe}^{\text{II}}(\text{phen})_2(\text{SCN})_2$  Discussed in the Text<sup>a</sup>

matrix	KBr	KBr	KBr	KBr
temp/K	300	80	8	78
form	HS-1	LS-1	HS-2	LS-2
band				
$\alpha$ (CCC)	637.6 (m)	645.3 (w)	638.5 (m)	645.3 (w)
$\gamma$ (CH)	725.3 (s)	720.5 (s)	725.3 (vs, br)	721.5 (s)
		724.4 (sh)		724 (sh)
	763.9 (m)	759.1 (m)	764 (w)	760 (m)
$\nu_3$ (CS)?	806.3 (w)	805.4 (s)	806.3 (m)	806.3 (m)
			809.2 (m)	809.2 (m)
$\gamma$ (CH)	846.9 (vs)	844 (vs)	845.9 (vs, br)	844.9 (vs)
	865.2 (m)	865 (vw)	867.1 (m)	866.4 (w)
$\nu_1$ (CN, as)	2062.2 (vs)		2068 (vs)	
$\nu_1$ (CN, s)	2072.8 (vs)		2077 (vs)	
$\nu_1$ (CN, as)		2106.5 (vs)		2106.5 (vs)
$\nu_1$ (CN, s)		2114.2 (vs)		2114.2 (vs)

<sup>a</sup>All values in  $\text{cm}^{-1}$ ; s = strong, m = medium, w = weak, sh = shoulder, v = very; br = broad.

have essentially disappeared at the lower temperature. It is clear from these results that the 900–600- $\text{cm}^{-1}$  region of the IR spectrum can also be used to establish the identity of the ferrous complex present under a given set of conditions. It is also to be noted from these data (although somewhat less precise than the data summarized in Figure 2 due to lower signal to noise ratio in the lower frequency band profiles) that the HS  $\rightleftharpoons$  LS conversion is again  $\sim 50\%$  complete at a temperature of  $153 \pm 2$  K, consistent with the  $\nu_{\text{CN}}$  band behavior discussed above but at variance with the transition temperatures as measured by other physicochemical techniques. As noted above, this difference in the apparent HS  $\rightleftharpoons$  LS transition temperature as monitored by different spectroscopic methods may arise from the sampling techniques employed in the infrared methods of this study. Further investigations of the apparent transition temperature dependence on pressure and dilution are currently underway.

With the characteristic IR absorptions due to the HS and LS forms of  $\text{Fe}(\text{phen})_2(\text{SCN})_2$  in mind, it is now possible to address the question of the identity of LS-1 and LS-2 on the one hand, and HS-1 and HS-2, on the other (see Figure 1). With respect to the former pair, careful comparison of the IR spectral features in both the 900–600- and 2200–1900- $\text{cm}^{-1}$  regions shows that the low-spin form of  $\text{Fe}(\text{phen})_2(\text{SCN})_2$  obtained by cooling the sample from room temperature to  $\sim 80$  K and that obtained by warming the optical-pumping-produced high-spin form from liquid-helium temperature to  $\sim 80$  K are completely identical. This conclusion is in consonance with the  $^{57}\text{Fe}$  Mössbauer data of Gutlich et al., who noted that sample heating at 55 K for short times causes the complex to relax gradually back to the low-spin state (with presumably identical Mössbauer parameters).

Comparison of HS-1 and HS-2, on the other hand, shows two distinct differences in the IR spectra. The first of these is the observation that the weak absorption at  $\sim 806 \text{ cm}^{-1}$  in HS-1 at 300 K has become significantly more intense in HS-2 at 8 K, being observed as a broad absorbance with overlapping peaks at 809 and  $806 \text{ cm}^{-1}$ . More dramatic is the position of the two cyanide moiety vibrations in the 2070- $\text{cm}^{-1}$  region. In HS-1, these absorption maxima are at 2062.2 and  $2072.8 \text{ cm}^{-1}$ , respectively, while in the HS-2 spectra (at  $\sim 8$  K), these maxima are located at 2068 and  $2076.6 \text{ cm}^{-1}$ , respectively (see Table I). To ensure that these blue shifts of 5.7 and  $3.8 \text{ cm}^{-1}$  do not originate in the temperature difference between the two samples, a careful study was undertaken to calibrate the temperature dependence of the HS-1 peak positions in the range  $80 \leq T \leq 300$  K. Within the accuracy of the present experimental arrangement ( $\pm 0.5 \text{ cm}^{-1}$ ), these two absorptions are temperature independent ( $2073.6 \pm 0.4 \text{ cm}^{-1}$ ) over the above temperature range. These results are in agreement with related studies<sup>26</sup> of the temperature dependence of  $\nu_{\text{CN}}$  in, for example, KSCN ( $2047.0 \pm 0.6 \text{ cm}^{-1}$ ,  $78 \leq T \leq 300$  K), and in contrast to those observed<sup>27</sup> for organometallic compounds containing the SCN group as a bridging ligand, in which the CN stretching frequency has a significant temperature dependence

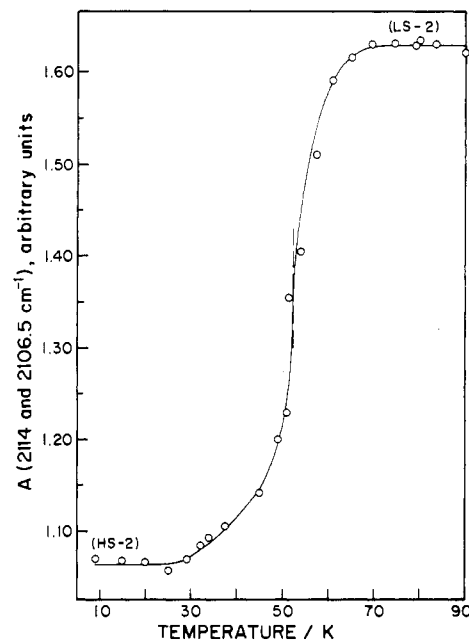


**Figure 7.** Temperature dependence of the sum of the infrared absorbances at 2114 and  $2106.5 \text{ cm}^{-1}$ , associated with the LS-2 form (see text and Figure 1) of  $\text{Fe}(\text{phen})_2(\text{SCN})_2$ . The vertical dashed line at  $55 \pm 1$  K shows the temperature at which the mean absorbance value in the range 9–90 K is reached. The starting “high-spin” form, HS-2, was obtained by LIESST pumping at 9 K by 632.8-nm radiation from the He/Ne laser of the spectrometer.

over the same interval. It is clear from these results that the differences in the infrared absorption maxima in HS-1 at 300 K and HS-2 at 8 K are not due to the differences in the sample temperature but originate in small but significant differences in the nature of the high-spin form of  $\text{Fe}(\text{phen})_2(\text{SCN})_2$  at room temperature and the high-spin form of this complex formed by the LIESST process near liquid-helium temperature. Again, this conclusion is supported by a comparison of the  $^{57}\text{Fe}$  Mössbauer data of Gutlich et al.,<sup>4</sup> who note that the isomer shift and quadrupole splitting of HS-1 at 4.2 K are 1.172 (13) and 3.233 (20)  $\text{mm s}^{-1}$ , respectively, while those of the LIESST-converted form at 6 K are 0.971 (7) and 3.01 (1)  $\text{mm s}^{-1}$ , respectively. Since the Mössbauer data pertain to neat samples of the ferrous complex while the IR data of the present study refer to dilute dispersions of the sample complex in several different matrices to give self-consistent results, it is clear that the observed differences in HS-1 and the LIESST-produced HS-2 are properties of the sample compound and not consequences of the sample preparation technique.

In fact, these observations are not at all surprising, since it is known both from structural and infrared data that there is an appreciable bond shortening in the metal–ligand interaction in going from the HS to the LS form. Thus, HS-2, formed by optical pumping at 8 K is expected to have a larger molecular volume than the LS-1 form of the matrix in which it is being produced. Effectively, the LIESST form HS-2 is subject to an internal “pressure” generated by this volume difference, and it is this compression that (presumably) accounts for the observed differences in the infrared spectra of HS-1 (300 K) and HS-2 (8 K) noted above.

**(c) The HS  $\rightarrow$  LS Conversion at  $T \leq 40$  K.** As noted from the  $^{57}\text{Fe}$  Mössbauer results cited above, the LIESST-produced high-spin form, which is trapped at temperatures near those of liquid helium, can be reconverted to the low-spin form by warming to temperatures of  $\sim 50$  K. This conversion is readily followed by the FTIR technique discussed in the present study, as summarized graphically in Figure 7. The initial decrease in LS absorption (and increase in the HS absorption) in the interval  $9 \leq T \leq 25$  K is due to continued LIESST conversion of the sample in the spectrometer due to He/Ne line irradiation as noted above. At  $\sim 50$  K, this process is overwhelmed by the thermally driven

HS  $\rightarrow$  LS conversion, which depopulates the HS form trapped in the matrix and converts the complex back into the LS species, which is the thermodynamically stable form at  $\sim 80$  K. The LIESST conversion at low temperatures and the subsequent "annealing" process at  $T > 40$  K are completely reversible, as shown by the fact that successive recycling of the sample through these temperature regimes produced closely replicate results. It may thus be concluded that the LIESST process does not depend on lattice defects produced by sample preparation methods but is, indeed, an intrinsic property of these spin-crossover complexes.

**Acknowledgment.** This research has been supported by a grant (DMR-8102940) from the Division of Materials Research of the National Science Foundation and the office of the Dean of the Faculty of Arts and Sciences of Rutgers University. The authors are indebted to Dr. J. E. Phillips for the electronic spectra cited in this study and to Profs. J. A. Potenza and H. J. Schugar for a number of illuminating discussions. We are also indebted to Prof. P. Gutlich for generously making available to us a sample of *cis*-Fe(phen)<sub>2</sub>(SCN)<sub>2</sub> used in his Mössbauer studies for comparison with the present infrared data.

Contribution from the Department of Chemistry,  
The University of Texas at Austin, Austin, Texas 78712

## Synthesis and Structures of Dinuclear Nickel(I) Di-*tert*-butylarsenido Complexes: X-ray Crystal Structures of [Ni( $\mu$ -*t*-Bu<sub>2</sub>As)(PMe<sub>3</sub>)<sub>2</sub>]<sub>2</sub> (Ni-Ni) and [Ni( $\mu$ -*t*-Bu<sub>2</sub>As)(CN-*p*-tol)<sub>2</sub>]<sub>2</sub> (Ni-Ni) (tol = Toly)

Richard A. Jones\* and Bruce R. Whittlesey

Received August 5, 1985

The reaction of NiCl<sub>2</sub>(PMe<sub>3</sub>)<sub>2</sub> with Li-*t*-Bu<sub>2</sub>As in THF at  $-78$  °C gives [Ni( $\mu$ -*t*-Bu<sub>2</sub>As)PMe<sub>3</sub>]<sub>2</sub> (**1**) in 37% yield. **1** reacts with excess *p*-tolyl isocyanide (CN-*p*-tol) in hexane at room temperature to give [Ni( $\mu$ -*t*-Bu<sub>2</sub>As)(CN-*p*-tol)<sub>2</sub>]<sub>2</sub> (**2**) in 47% yield. **1** and **2** are the first dinuclear diorganoarsenido complexes to be structurally characterized by X-ray diffraction. Crystal data for **1**: C<sub>22</sub>H<sub>54</sub>As<sub>2</sub>Ni<sub>2</sub>P<sub>2</sub>,  $M_r = 647.89$ , monoclinic,  $I2/a$  (a nonstandard setting of  $C2/c$ , No. 15),  $a = 16.848$  (3) Å,  $b = 12.069$  (1) Å,  $c = 17.379$  (3) Å,  $\beta = 114.60$  (2)°,  $U = 3213.2$  (5) Å<sup>3</sup>,  $D_{\text{calcd}} = 1.339$  g cm<sup>-3</sup>,  $Z = 4$ ,  $\lambda(\text{Mo K}\alpha) = 0.71069$  Å (graphite monochromator),  $\mu(\text{Mo K}\alpha) = 33.24$  cm<sup>-1</sup>, final  $R = 0.0399$  ( $R_w = 0.0526$ ) from 2245 observed reflections ( $I > 3\sigma(I)$ ), 2433 measured. Crystal data for **2**: C<sub>48</sub>H<sub>64</sub>As<sub>2</sub>Ni<sub>2</sub>N<sub>4</sub>,  $M_r = 964.34$ , monoclinic,  $P2_1/n$  (a nonstandard setting of  $P2_1/c$ , No. 14),  $a = 13.320$  (2) Å,  $b = 12.889$  (2) Å,  $c = 15.042$  (3) Å,  $\beta = 111.00$  (2)°,  $V = 2410.7$  (5) Å<sup>3</sup>,  $D_{\text{calcd}} = 1.328$  g cm<sup>-3</sup>,  $Z = 2$ ,  $\lambda(\text{Mo K}\alpha) = 0.71069$  Å (graphite monochromator),  $\mu(\text{Mo K}\alpha) = 21.78$  cm<sup>-1</sup>, final  $R = 0.0563$  ( $R_w = 0.0657$ ) from 1557 observed reflections ( $I > 3\sigma(I)$ ), 1743 measured. **1** contains two 16-electron Ni(I) atoms bridged by two *t*-Bu<sub>2</sub>As groups and linked by a single Ni-Ni bond (Ni-Ni = 2.429 (1) Å). A crystallographically imposed twofold axis passes through each As atom, giving a planar symmetrical central Ni<sub>2</sub>As<sub>2</sub> core. Each Ni atom bears a PMe<sub>3</sub> group, which is virtually coplanar with the Ni<sub>2</sub>As<sub>2</sub> plane. In **2** the CN-*p*-tol groups give each Ni atom a pseudotetrahedral geometry. The central Ni<sub>2</sub>As<sub>2</sub> core is again planar by virtue of a crystallographic center of inversion, which lies at the midpoint of the Ni-Ni bond (Ni-Ni = 2.693 (2) Å). Trends in Ni-Ni bond lengths in these and related complexes are correlated with the electron count on the metal centers and the type of bridging atom.

### Introduction

Although there are a number of compounds in which two nickel atoms are linked by dialkylphosphide bridges, there are only two examples of similar complexes containing dialkylarsenido ligands. Neither of these have been characterized crystallographically. The first such compound was [CpNi( $\mu$ -AsMe<sub>2</sub>)<sub>2</sub>]<sub>2</sub>, which was reported by Hayter<sup>1</sup> in 1963 and which presumably does not contain a nickel-nickel bond. Shortly thereafter, the complex [NiCl(NO)( $\mu$ -AsPh<sub>2</sub>)<sub>2</sub>]<sub>2</sub> was synthesized by Kumar and Hieber.<sup>2</sup> Both compounds contain 18-electron nickel atoms in a formal oxidation state of +2. In addition, several heterobimetallic dimethylarsenido-bridged complexes containing nickel have been made, namely, Cp(CO)<sub>*n*</sub>M( $\mu$ -AsMe<sub>2</sub>)Ni(CO)<sub>3</sub> ( $n = 3$ , M = Cr, Mo<sup>3</sup>, W;<sup>4</sup>  $n = 2$ , M = Fe<sup>5</sup>). This paper describes the syntheses and crystal structures of [Ni( $\mu$ -As(*t*-Bu)<sub>2</sub>)(PMe<sub>3</sub>)<sub>2</sub>]<sub>2</sub> (**1**) and [Ni( $\mu$ -As(*t*-Bu)<sub>2</sub>)(CN-*p*-tol)<sub>2</sub>]<sub>2</sub> (**2**), which are the first nickel dialkylarsenido complexes to be structurally characterized.

### Results and Discussion

[Ni( $\mu$ -*t*-Bu<sub>2</sub>As)(PMe<sub>3</sub>)<sub>2</sub>]<sub>2</sub> (Ni-Ni) (**1**). The interaction of NiCl<sub>2</sub>(PMe<sub>3</sub>)<sub>2</sub> with 2 equiv of *t*-Bu<sub>2</sub>AsLi in THF at  $-78$  °C gives a dark red solution from which black crystals of [Ni( $\mu$ -*t*-Bu<sub>2</sub>As)(PMe<sub>3</sub>)<sub>2</sub>]<sub>2</sub> (**1**) may be isolated in ca. 37% yield. The complex is air-stable for short periods in the solid state but de-

composes rapidly in solution when exposed to the air. NMR spectroscopic data (<sup>1</sup>H and <sup>31</sup>P) is consistent with the solid-state structure as determined by an X-ray diffraction study. The <sup>1</sup>H NMR shows signals at  $\delta$  1.43 and 1.39 (relative to Me<sub>4</sub>Si,  $\delta$  0.0) attributable to the PMe<sub>3</sub> and *t*-Bu groups, respectively. The <sup>31</sup>P{<sup>1</sup>H} NMR spectrum shows a singlet  $\delta$  20.48 for the PMe<sub>3</sub> ligands. **1** reacts with 2 equiv of I<sub>2</sub> in toluene at room temperature to give *trans*-Ni(PMe<sub>3</sub>)<sub>2</sub>I<sub>2</sub>. The crystal structure of this complex has been determined, and it will be described elsewhere.

**X-ray Structure of 1.** The complex crystallizes in the monoclinic space group  $I2/a$  (a nonstandard setting of  $C2/c$ , No. 15) with half a molecule in the asymmetric unit (four per unit cell). Crystal data and the summary of intensity data collection parameters for **1** are given in Table I. Atomic positional parameters, bond lengths, and bond angles for **1** are presented in Tables II-IV, respectively. A general view of the molecule with the atom-numbering scheme is shown in Figure 1. The structure consists of discrete molecules with no short intermolecular contacts. The As atoms lie on a crystallographically imposed twofold axis, giving the central Ni<sub>2</sub>As<sub>2</sub> core a planar geometry. The terminal PMe<sub>3</sub> ligands are arranged so that the Me<sub>3</sub>P-Ni-Ni-PMe<sub>3</sub> unit is virtually linear (P-Ni-Ni = P'-Ni'-Ni = 179.37 (3)° giving the molecule a virtually  $D_{2h}$  symmetry. The Ni-Ni distance of 2.429 (1) Å is in accord with a single metal-metal bond, giving each Ni atom an unsaturated 16-electron configuration. This distance is somewhat larger than that found in the *t*-Bu<sub>2</sub>P analogue of **1** (2.375 (3) Å), which we recently described.<sup>6</sup> The reason for this

(1) (CpNiAsMe<sub>2</sub>)<sub>2</sub>: Hayter, R. G. *Inorg. Chem.* **1962**, *2*, 1031.

(2) (NiCl(NO)AsPh<sub>2</sub>)<sub>2</sub>: Hieber, W.; Kummer, R. *Z. Anorg. Allg. Chem.* **1966**, *344*, 292.

(3) Madach, T.; Vahrenkamp, H. *Z. Naturforsch., B: Anorg. Chem., Org. Chem.* **1979**, *34*, 1195.

(4) Panster, P.; Malisch, W. *Chem. Ber.* **1976**, *109*, 3842.

(5) Müller, R.; Vahrenkamp, H. *Chem. Ber.* **1977**, *110*, 3910.

(6) Jones, R. A.; Stuart, A. L.; Atwood, J. L.; Hunter, W. E.; Rogers, R. D. *Organometallics* **1982**, *1*, 1721. Jones, R. A.; Stuart, A. L.; Atwood, J. L.; Hunter, W. E. *Organometallics* **1983**, *2*, 874.